Influence of Intermediate Hinge Damage on Bridge Response and Modal Parameters of Cantilever-Suspended Girder Bridge

Aoi Hiraoka, Gen Hayashi & Takashi Yamaguchi

Citation	European Workshop on Structural Health Monitoring. 2022; 745-753.
Book series	Lecture Notes in Civil Engineering, vol 254.
Published	2022-06-16
Type	Conference paper
Textversion	Author
Rights	© 2023 The Author(s), under exclusive license to Springer Nature Switzerland AG. For Academic research only. This is the accepted manuscript version. The formal published version is available at https://doi.org/10.1007/978-3-031-07258-1_75. See Springer Nature Accepted Manuscript Terms of Use: https://www.springernature.com/gp/open-research/policies/accepted-manuscript-terms
DOI	10.1007/978-3-031-07258-1_75

Hiraoka, A., Hayashi, G., Yamaguchi, T. (2023). Influence of Intermediate Hinge Damage on Bridge Response and Modal Parameters of Cantilever-Suspended Girder Bridge. In: Rizzo, P., Milazzo, A. (eds) European Workshop on Structural Health Monitoring. EWSHM 2022. Lecture Notes in Civil Engineering, vol 254. Springer, Cham. https://doi.org/10.1007/978-3-031-07258-1_75

Influence of Intermediate Hinge Damage on Bridge Response and Modal Parameters of Cantilever-Suspended Girder Bridge

Aoi Hiraoka[1], Gen Hayashi[2], and Takashi Yamaguchi[2]

[1]Osaka City Univ. 3-3-138 Sugimoto Sumiyoshi-ku, Osaka 558-8585 JAPAN
hiraoka@brdg.civil.eng.osaka-cu.ac.jp
[2] Osaka City Univ. 3-3-138 Sugimoto Sumiyoshi-ku, Osaka 558-8585 JAPAN
hayashi-g@osaka-cu.ac.jp

Abstract. Cantilever-suspended girder bridges are provided with intermediate hinges to reduce the effects of support settlement, including damage to hinge bearings caused by corrosion. To inspect, repair, and efficiently maintain these bridges, it is necessary to develop a monitoring technology. Accordingly, research have been conducted on a bridge response health-monitoring technology. In particular, the properties of bearings significantly influence the vibration characteristics of bridges. However, previous studies are yet to examine changes in bridge response due to the corrosion of hinge bearings. Using finite element analysis (FEA), this study aimed to investigate changes in the bridge response and modal parameters of cantilever-suspended girder bridges due to the corrosion damage levels of the hinge bearings. In the FEA, model-installed elastic spring was used shell elements. Furthermore, static and eigenvalue analyses were conducted. Static analysis demonstrated that the target bridge type exhibited more minor changes in its girder deflection due to bearing corrosion. In addition, the effects were quantitatively determined by altering the corrosion position of the hinge bearing in the bridge.

Keywords: Cantilever-suspended Girder Bridge, Hinge Bearing, Corrosion, Bridge Health Monitoring

1 Introduction

Several bridges in Japan were constructed five decades ago. Considering that the number of bridges will continuously increase in the future, the maintenance of aging bridges is a crucial issue. Hence, the revision of periodic inspection guidelines for bridges in Japan has made it necessary for road bridge inspections to be conducted periodically[1)]. However, the maintenance of these bridges has been conducted by engineers with specialized knowledge of visual and percussion inspections, which creates certain problems such as high human costs, shortage of engineers, and inspection inefficiencies.

Bridge health monitoring (BHM) is expected to be an efficient maintenance method. BHM is a technology that evaluates performance and determines the existence of damage to a bridge based on the response of the bridge to various sensors placed on the bridge. In particular, damage detection by vibration-based health monitoring (VSHM) adopts acceleration response. In previous studies, VSHM was applied to various steel bridges such as truss, arch, and girder bridges[2)–6)]. However, it is difficult to repair or replace an existing bridge based on changes in its vibration characteristics alone. Therefore, BHM applications must consider the load-carrying capacity, which is important in decision-making regarding vibration characteristics.

This study focused on a cantilever-suspended girder bridge, which is yet to be studied. Cantilever-suspended girder bridges are provided with intermediate hinges to reduce the effects of support settlement, and damage to hinge bearings caused by corrosion has been reported. However, previous studies are yet to examine changes in the vibration characteristics and load-carrying capacity due to the corrosion of hinge bearings.

In this study, to examine the applicability of the BHM technology, the effects of the location of the corroded hinges and corrosion level on the response of the bridge were investigated analytically. Subsequently, the relationship between the vibration characteristics and the static response was clarified via eigenvalue analyses and static analyses.

2 Actual target bridge and analysis model

2.1 Actual target bridge

The actual target bridge, which was completed in 1959, is a cantilever-suspended non-synthetic girder bridge with seven spans, including suspended-span and cantilever-girder lengths of 16.0 m and 40.8 m (6.2 m + 28.4 m + 6.2 m), respectively. Because the target bridge is symmetrical, its general drawing can be obtained from the A2 abutment to its center, as illustrated in Fig. 1. The bridge bears a large amount of heavy vehicular traffic daily. In the past, the slabs and main girders of its hinges were reinforced by a steel plate to prevent fatigue cracking.

2.2 Finite element method (FEM)

In this study, entire bridge overviews of the models are presented in Fig. 2. The general-purpose FEM software Abaqus/Standard 2020 was used for the analysis. To develop the model, the main load transfer members, which include the slab, main girder, stringer beam, and cross beam were modeled. The dimensions adopted are presented in Table 1 and Fig. 3. The elastic moduli of the slab and girders were 30 GPa and 200 GPa, respectively. The boundary conditions were modeled as linear springs resisting the vertical and two horizontal directions so as to represent the rubber bearing of the bridge, as illustrated in Fig. 4. The spring constants were set as 1450 MN/m and 3.32 MN/m in the vertical and horizontal directions, respectively. The spring constant was calculated

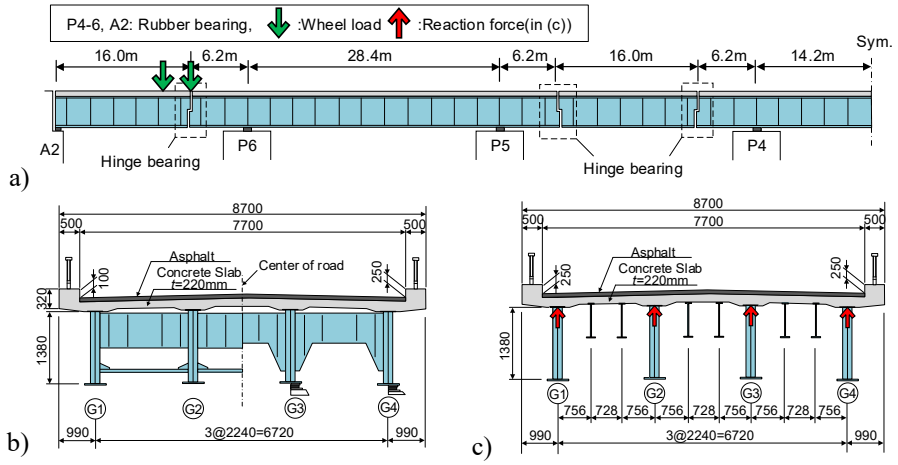

Fig. 1. General drawing of the actual bridge: (a) side view; (b) sectional view (girder end); and (c) sectional view (the central part)

based on the road bridge bearing handbook[7]. In the eigenvalue analysis, the masses of the bridge were given as the material properties and densities of the members. The slab density was 23 kg/m^3, while that of the girders was 77 kg/m^3.

2.3 Finite element analysis (FEA) model

All the members were modeled using four-node reduced-integral shell elements in the shell model. The element size was set to 100 mm × 100 mm for all the members. Fig. 5(b) and (c) present the method for modeling and constraining the hinges. In this model, the reference points were set to the top surface of the upper flange in the main cantilever span and the bottom surface of the lower flange in the suspended span of the half-joint. These sets were joined to two nodes placed in the middle of the upper and lower surfaces of the half-joint. The double nodes are represented by pinning the two nodes.

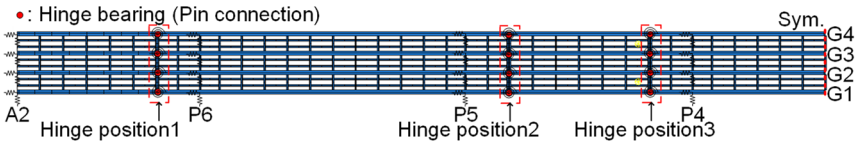

Fig. 2. Overview of the entire bridge modeled using shell elements.

Table 1. Dimensions of members

Member	Shape	Dimension (Unit: mm)
Slab		$B = 8700$, $h_d = 220$
Main girder	I	Upper flange: $B_{uf} = 400$, $t_{uf} = 28$ Web: $h_g = 1380$, $t_w = 9$ Lower flange: $B_{uf} = 440$, $t_{uf} = 32$
Crossbeam, stringer beam	I	Upper flange, Lower flange: $B_{uf} = 200$, $t_{uf} = 10$ Web: $h_g = 630$, $t_w = 9$

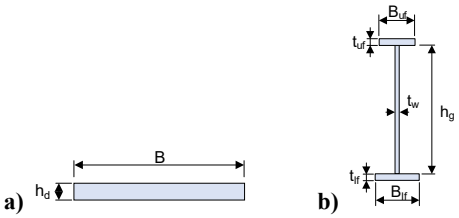

Fig. 3. Member section: (a) slab; and (b) girder

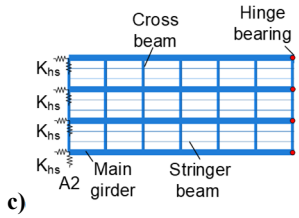

Fig. 4. Rubber bearing of the model

2.4 Loading method and damage modeling

The load adopted for static analysis is a wheel load equivalent to the designed actual load mentioned in the Specifications for Highway Bridges (front axle weight: 122.6 kN; rear axle weight: 122.6 kN). The distance between the front and rear axle weights was 3.88 m for an actual vehicle. The loading position was at the top of the upper flange of the main girder, just above the hinge in the end-suspended span section (hinge position 1 in Fig.2). The load distributed across the four main girders was calculated and loaded on each girder, assuming that the loading truck traveled in the center of one lane, as illustrated in Fig. 1. In the analysis conducted on the sensitivity of the hinges to corrosion, it is necessary to represent the corrosion of the hinges. Therefore, an elastic rotational spring resisting at a position perpendicular to the bridge axis was introduced to the hinges, and the corrosion was simulated by altering the spring constant.

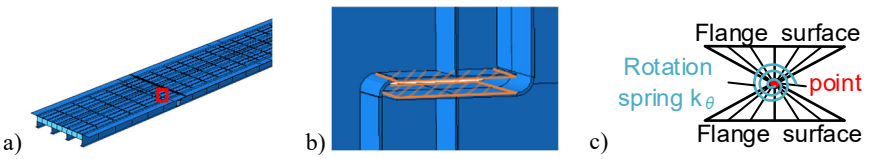

Fig. 5. Overview of the shell model: (a) entire view; (b) hinge bearing part; and (c) image of the hinge model

3 Effect of corrosion position

3.1 Analysis conditions

The relationship between the vibration characteristics and bridge response when the location of the corroded hinge was altered was investigated. This section examines the change in the natural frequency when the spring constant increases by introducing springs in all hinges. Fig. 6 presents the sensitivity analysis results. The hinge was intact when the spring constant was small, thereby implying a rotational support. Conversely, the hinge was corroded when the spring constant was large, thus implying a fixed state. From Fig. 6, a transition interval is observed between the spring constants k = 10^7 Nmm and 10^{14} Nmm.

Analysis results for this bridge retains the behavior of the cantilever-suspended girder bridge even when the spring constant of the hinge spring increases, because the hinge is locally constrained. Therefore, this model accurately captures the behavior of the actual bridge used in subsequent investigations. The analysis cases to be considered when altering the corroded hinge position are presented in Table 2 and Fig. 2. In Table 2, the number following the "s" in the case name indicates the corroded position. The number of corrosion locations under the hinges is presented in Fig. 2. The following letters indicate the hinges in girders G1–G4 that were corroded. Eigenvalue and static analyses were performed for the 12 cases.

3.2 Eigenvalue analysis

The eigenvalue analysis results for the 12 analyzed cases are presented in Fig. 7. The maximum changes between the intact and fixed states of the first and second bending modes of the first torsional mode were approximately 0.07 Hz and 0.20 Hz, respectively; in case of the second torsional mode, the values were 0.01 Hz and 0.07 Hz, respectively. The most significant change was observed in the second bending mode, whereas the changes in the other modes were negligible (less than 0.1 Hz). Focusing on the second bending mode, the difference in case-s2-all between the intact and fixed states was approximately 0.1 Hz, which is the next most significant change after case-s123-all. case-s2-all corroded all bearings at hinge position-2. Hence, the changes in

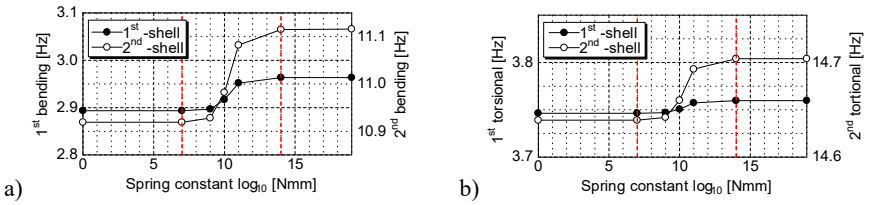

Fig. 6. Relationship between spring constant and natural frequency during total hinge corrosion: (a) bending mode; and (b) torsional mode

Table 2. Analysis case

Case name	S123 -all	S1 -all	S2 -all	S3 -all	S123 -G1G4	S12 -G1G4	S23 -G1G4	S1 -G1G4	S2 -G1G4	S3 -G1G4	S1 -G4	S2 -G4
Corroded position	1,2,3	1	2	3	1,2,3	1,2	2,3	1	2	3	1	2
Corroded bearing	all	all	all	all	G1G4	G1G4	G1G4	G1G4	G1G4	G1G4	G4	G4

case-s123-G1G4, case-s23-G1G4, and case-s3-all were relatively large at approximately 0.1 Hz.

In contrast, case-s1-all exhibited the least change among all cases. From these results, corroded hinge position-2 and position-3, which bear the suspended span, tend to emerge in the natural frequency. This is because the intermediate suspended span is where the modes tend to dominate, as shown in Fig.8. The bending mode shapes oscillated most dominantly at the mid-suspended span. A simple girder supported this span on top of the overhanging beams on both sides. Hence, the vibration mode of this span is dominant owing to the vibration of the anchorage span on both sides compared with the end-suspended span, where one end is located on the bearing, as illustrated in Fig. 8.

Moreover, comparing the amount of change in case-a2-all, case-a2-G1G4, and case-a2-G4 from the intact state yielded values of approximately 0.1 Hz, 0.05 Hz, and 0.25 Hz, respectively. The number of corroded hinges is proportional to the frequency of the second bending mode. This is because the second bending mode shape dominates at both the hinges of the intermediate suspension girder, as illustrated in Fig. 8.

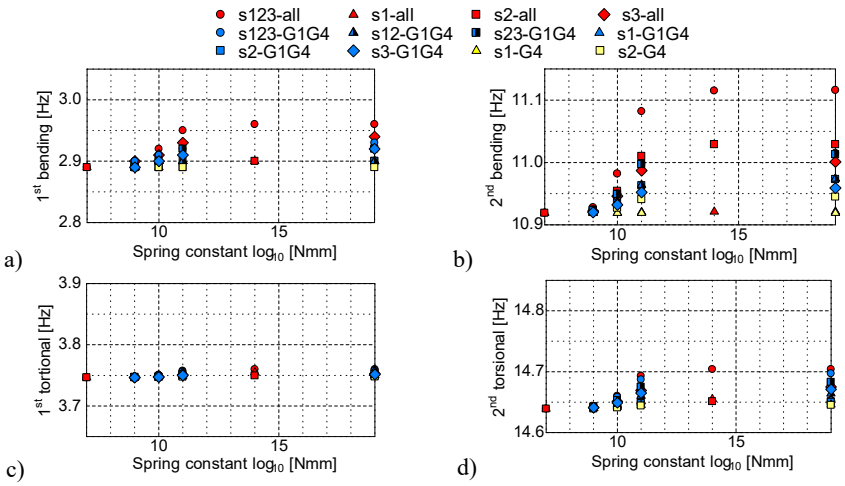

Fig. 7. Results of eigenvalue analysis: (a) 1st bending mode; (b) 2nd bending mode; (c) 1st torsional mode; and (d) 2nd torsional mode

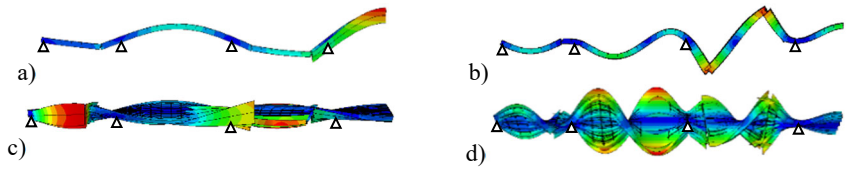

Fig. 8. Mode shape of the shell model: (a)1st bending mode (shell); (b) 2nd bending mode; (c) 1st torsional mode (shell); (d) 2nd torsional mode (shell).

3.3 Static analysis

Fig. 9 presents the static analysis results for the 12 cases. The vertical deflection was measured at the bottom surface under the lower flange, directly below hinge position-1 of G4. In all the analysis cases, the vertical deflection was smaller than that in the intact state. Consequently, the rotation is restricted by the spring at the hinge, stiffness increases, while deflection decreases.

In case-s123-all, the change between the intact and fixed states was the most significant, 0.38 mm, followed by case-s1-all, where the change was 0.35 mm. The difference in change between cases-s1-all and cases-s123-all was 0.03 mm. This indicates that the change in hinge properties at the loading position is primarily responsible for the response change. This is because the restriction of the rotating spring increased as the deformation increased. The cases with the largest amount of change are case-s1-all, case-s123-G1G4, case-s12-G1G4, and case-s1-G4.

3.4 Relationship between frequency and deflection

The correlation between the eigenvalue analysis results in Section 3.2 and the static analysis results in Section 3.3 is discussed in this subsection. Fig.10 presents the relationship between the vertical deflection and second bending mode with the most

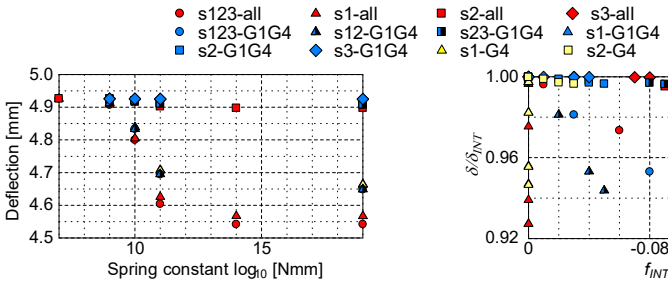

Fig. 9. Results of static analysis

Fig. 10. Relationship between the natural frequency of the 2nd bending mode and deflections

significant change in natural frequency due to the spring constant. The horizontal axis of Fig. 10 represents the difference between the natural frequency of the intact state and the natural frequency of each case, while the vertical axis denotes the deflection of each case divided by the deflection of the intact state—a nondimensional quantity.

The vertical deflection changed significantly when the spring was introduced at hinge position-1, just below the loading position. However, the natural frequency changed significantly in the case of the spring presented at hinge position-2 and position-3, which are the bearings of the suspended span. Consequently, the corrosion of the hinges in the middle-suspended span was detected based on the change in the natural frequency of the second bending mode. Furthermore, the difference in the deflections due to direct loading indicated the corrosion of the hinges of the end suspension girder.

4 Summary

Differences in vibration and static characteristics of cantilever-suspended girder bridges due to the corrosion damage of the hinge bearings were investigated using FEA modeling; the effects of the locations of the corroded hinges and corrosion levels on the response of the bridge were analytically studied for the constructed model.

1. The change in the natural frequency due to corroded bearing at all locations is about 0.2 Hz in the second bending mode among all vibration modes. In the case of partial corroded bearing, the natural frequency change is about 0.12Hz in the corroded bearing at the suspended span. In contrast, the no change in natural frequency with the corrosion of the end-suspended span bearing.
2. The deflection just below the target hinge bearing is about 0.3 mm smaller than intact case when a direct load is applied to a corroded hinge.
3. In the case of corroded bearing in suspended span, the natural frequency and deflection are correlated.
4. In the future, the relationship between corrosion and bridge response clarify by moving load analysis, the effective parameters for BHM investigate.

Acknowledgements

This work was supported by Grants-in-Aid for Ueda Memorial Foundation

Reference

1. Road Bureau, MLIT, https://www.mlit.go.jp/road/sisaku/yobohozen/tenken/yobo4_1.pdf, last accessed 2022/2/22.
2. Wickramasinghe, W.R., Thambiratnam, D.P., Chan, T.H.T, Nguyen, T.: Vibration characteristics and damage detection in a suspension bridge. In: Journal of Sound and Vibration, Vol.375, pp.254-274 (2016).
3. Chang, K.C., Kim, C.W.: Modal-parameter identification and vibration-based damage detection of a damaged steel truss bridge. In: Engineering Structures, pp.156-173 (2016).

4. Kim, C.W., Chang, K. C., Kitauchi, S., McGetrick, P.: A field experiment on a steel Gerber-truss bridge for damage detection utilizing vehicle-induced vibrations. In: Structural Health Monitoring (SHM), Vol.15, Issue2, pp.174-192 (2016).
5. Kim, C.W., Mimasu, T., Goi Y., Hayashi G.: Investigations on increase and decrease of frequencies of a steel plate girder bridge due to artificial cracks. In: 9th International conference on Structural Health Monitoring of intelligent Infrastructure (SHMII), Vol.1, pp.689-694 (2019).
6. Kim, C.W., Luna Vera, O.S., Kondo, Y., Oshima, Y.: Vibration monitoring on a PC girder bridge during a bridge collapse test. In: 13th International Conference on Applications of Statistics and Probability in Civil Engineering, ICASP13, pp.1-8 (2019).
7. Japan Road Association: Road Bridge Bearing Handbook, (2018).